Chemical Physics Letters 633 (2015) 214–217

Contents lists available at ScienceDirect

Chemical Physics Letters

journal homepage: www.elsevier.com/locate/cplett

Editor's Choice

The hydration structure of dissolved carbon dioxide from X-ray absorption spectroscopy

Royce K. Lam[a,b], Alice H. England[a,b,1], Jacob W. Smith[a,b], Anthony M. Rizzuto[a,b], Orion Shih[a,2], David Prendergast[c], Richard J. Saykally[a,b,*]

[a] Department of Chemistry, University of California, Berkeley, CA 94720, USA
[b] Chemical Sciences Division, Lawrence Berkeley National Laboratory, Berkeley, CA 94720, USA
[c] Molecular Foundry, Lawrence Berkeley National Laboratory, Berkeley, CA 94720, USA

ARTICLE INFO

Article history:
Received 15 April 2015
In final form 20 May 2015
Available online 3 June 2015

ABSTRACT

The dissolution of carbon dioxide in water and its subsequent hydrolysis reactions comprise one of the most central processes in all of science, yet it remains incompletely understood despite enormous effort. We report the detailed characterization of dissolved CO_2 gas through the combination of X-ray spectroscopy and first principles theory. The molecule acts as a hydrophobe in water with an average hydrogen bond number of 0.56. The carbon atom interacts weakly with a single water at a distance of >2.67 Å and the carbonyl oxygens serve as weak hydrogen bond acceptors, thus locally enhancing the tetrahedral water hydrogen bonding structure.

Published by Elsevier B.V.

1. Introduction

The dissolution of carbon dioxide in water and its subsequent hydrolysis reactions comprise one of the most central processes in all of science [1–13], yet it remains incompletely understood despite enormous effort [14]. The solubility of gaseous CO_2 is governed by Henry's Law under equilibrium conditions ($k_H = 3.38 \times 10^{-2}$ mol L^{-1} atm^{-1}), with normal average CO_2 pressures in the atmosphere (3.9×10^{-4} atm) yielding total dissolved CO_2 concentrations of 1.33×10^{-5} M in pure water [14]. Most of this is present as the weakly hydrated CO_2 molecule, but a small fraction (~1%) hydrolyzes to form the short-lived carbonic acid (H_2CO_3) molecule, which subsequently forms bicarbonate, and carbonate ions via proton transfer reactions [15–17].

The chemical reaction of CO_2 with water to form carbonic acid is clearly the central feature of these carbonate equilibria, and has been addressed by many experiments [5,16,18–26] and calculations [17,27–36] with conflicting results. Details of the neutral CO_2 solvation by bulk water prepare the reaction pathway, and are thus a determining factor in this chemistry.

We previously characterized the hydration structures of aqueous carbonate and bicarbonate using X-ray absorption spectroscopy [37]. More recently, we described the use of a fast-flowing liquid microjet mixing system to protonate a bicarbonate solution to generate the short-lived ($k = 26.3$ s^{-1}, $t_{1/2} \sim 26$ ms) carbonic acid molecule [22,38], which was subsequently probed by soft X-ray absorption spectroscopy. Interpretation of the measured spectra via first principles theory provided a detailed picture of the hydration of the acid as donating two strong hydrogen bonds to solvating waters while acting as a weak acceptor of one such bond [39]. Here we apply this same approach to study the hydration of dissolved carbon dioxide, providing the first experimental characterization of the solvated neutral molecule.

2. Experimental

2.1. Sample preparation

Samples (1 M $NaHCO_3$ and 1 M HCl) were prepared using 18.2 MΩ cm resistivity water obtained from a Millipore purification system. Concentrated HCl (12.1 M) was obtained from J.T. Baker. $NaHCO_3$ (>99.7% purity) was obtained from Macron Fine Chemicals. Samples were used without further purification.

2.2. Experimental design

Carbon K-edge total electron yield (TEY) spectra were collected at Beamline 8.0.1. A detailed description of the experimental setup

* Corresponding author at: Department of Chemistry, D31 Hildebrand Hall, University of California, Berkeley, CA 94720, USA.
E-mail address: saykally@berkeley.edu (R.J. Saykally).
[1] Present address: Oregon Health and Science University, Portland, OR 97207, USA.
[2] Present address: National Synchrotron Radiation Research Center, Hsinchu 30076, Taiwan.

http://dx.doi.org/10.1016/j.cplett.2015.05.039
0009-2614/Published by Elsevier B.V.

has been published previously [40]. A high flux (>10^{11} photons/s), high resolution ($E/\Delta E = 7000$), tunable soft X-ray beam is generated from an undulator at the Advanced Light Source (ALS), Lawrence Berkeley National Lab (LBNL). A dual syringe pump system (Teledyne-ISCO 260D) drives the two solutions through the fast-flow liquid mixing system and into a 50 μm ID capillary to generate the liquid microjet. The X-ray beam is focused (100 × 35 μm spot size) onto the jet in a high vacuum chamber (~2 × 10− torr). The liquid jet then passes through a skimmer and freezes onto a cryogenic (liquid nitrogen) trap. The TEY signal is collected as a function of photon energy (0.05 eV step size) using a biased copper electrode (2.1 kV) positioned ~1 cm above the jet. Vapor phase TEY spectra were measured by positioning the microjet a few mm above or below the liquid stream. Measured TEY spectra were processed using the finite impulse response (FIR) Fourier filtering algorithm in Igor Pro (Wavemetrics) to remove the high frequency background introduced by the liquid microjet mixing system.

2.3. Simulations and calculations

The molecular dynamics (MD) simulations and calculated X-ray absorption spectra were published previously [37,39]. Briefly, Amber 9 [41] was used to generate 10 ns classical NVT-MD trajectories for gaseous and dissolved CO_2 and Quantum mechanics/molecular mechanics (QM/MM) trajectories for carbonic acid. The simulation box for the aqueous species contained ~90 TIP3P water molecules. 100 uncorrelated snapshots were taken from each trajectory for use in the spectral calculation.

X-ray absorption spectra were calculated using the eXcited electron and Core Hole (XCH) density function theory (DFT) method [42]. Under the XCH approximation, the lowest energy core-hole excited state is treated explicitly while the higher excited states are generated from the resulting self-consistent field. The electronic structure was calculated using PWSCF from the Quantum-ESPRESSO package [43] and the PBE exchange correlation functional under the generalized gradient approximation was used to calculate the exchange correlation energy [44]. A plane wave basis set, employing the Vanderbilt Ultra-Soft Pseudopotential [46], with a 25 Ry kinetic energy cutoff and periodic boundary conditions was used to model the localized and delocalized states. The resulting calculated spectra were aligned relative to one another using the atomic alignment scheme developed previously wherein the calculated excitation energy is aligned with respect to that of an isolated carbon atom [37]. The calculated spectrum for CO_2 was then aligned to the corresponding C(1s)→π^* peak of gas phase CO_2. All other calculated spectra were aligned relative to that.

Calculated Radial Distribution Functions (RDFs) were generated using VMD Molecular Graphics Viewer [45].

3. Results and discussion

Using the fast-flow liquid microjet mixing system, the X-ray absorption spectra of a 1:1 acid:bicarbonate mixture was measured following three different interaction times, controlled by altering both the length of the silica capillary used to form the microjet and the volumetric flow rate. The X-ray absorption spectra of the C(1s)→π^* transition measured at the different mixing times are shown in Figure 1. As the interaction time between the acid and bicarbonate increases, a small, but measurable, blue shift (~0.05–0.1 eV) is observed. The spectrum shown in black corresponds to the shortest interaction time (~0.5 ms) and was assigned to aqueous carbonic acid ($k = 26.3\ s^{-1}$). At this shorter time, only a small amount (~1.3%) of the carbonic acid generated via the protonation of bicarbonate ($k_{on} = 4.7 \times 10^{10}\ M^{-1}\ s^{-1}$) has decomposed

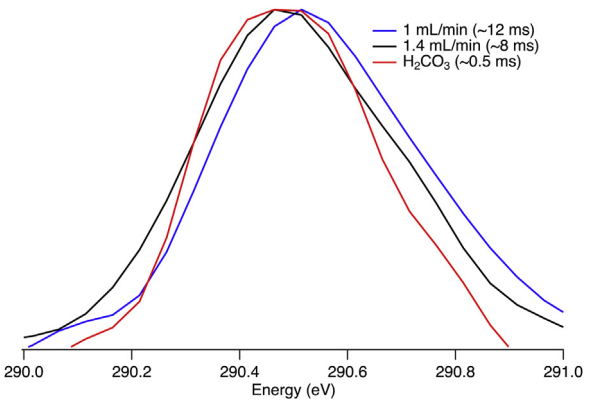

Figure 1. Peak-normalized experimental carbon K-edge X-ray aborption spectra of the C(1)→π^* transition of 1:1 HCl:$NaHCO_3$ mixtures at different interaction times. The absorption maxima are at 290.5 eV (H_2CO_3, ~0.5 ms), 290.5 eV (1 mL/min, ~8 ms), and 290.66 eV (1.4 mL/min, ~12 ms). All spectra were measured using a step size of 0.05 eV with samples introduced by the fast-flow microjet mixing system.

into dissolved carbon dioxide and water ($k = 26.3\ s^{-1}$) [22,38]. To lengthen the time before measuring the X-ray absorption spectrum, a 10 cm long, 50 μm ID silica capillary was used at two different flow rates (1.4 mL/min and 1.0 mL/min) which corresponds to an interaction time of ~8 and ~12 ms respectively. With the increased interaction time, significantly larger amounts, ~19% and 27% of the initial 0.5 M aqueous carbonic acid concentration, of carbon dioxide should be present.

While gaseous carbon dioxide exhibits a weak vibronic peak at ~292.8 eV, dissolved carbon dioxide does not. As shown in Figure 2, the vibronic peak is not present in the spectra measured following the longer interaction times, indicating that the observed blueshift is a result of the presence of dissolved, rather than gaseous, carbon dioxide. The observed blueshift is also consistent with predictions from theory. The calculated C(1s)→π^* transition (Figure 3) of dissolved carbon dioxide exhibits a small (~0.4 eV) blueshift from that of carbonic acid and is slightly redshifted (~0.7 eV) from that of gaseous carbon dioxide.

The solvation structure of dissolved CO_2 has been addressed by molecular dynamics simulations. From snapshots generated from the MD simulations, we find the average hydrogen bond number of CO_2, measured to a distance of 2.5 Å, to be 0.56 *vs* 3.17 for H_2CO_3, indicating that dissolved CO_2 is poor hydrogen bond acceptor and is extremely weakly hydrated. The radial distribution

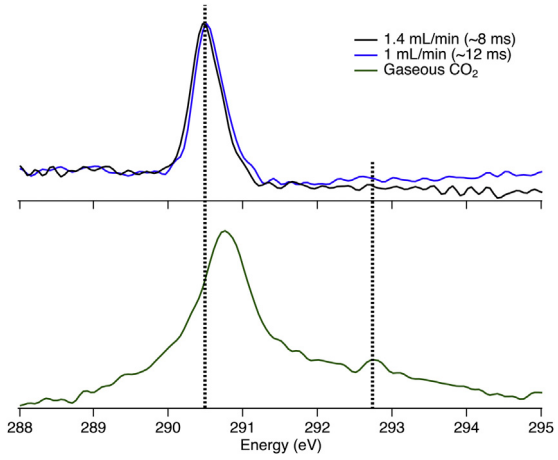

Figure 2. Comparison between XAS spectra of 1:1 HCl:$NaHCO_3$ mixtures at ~8 and ~12 ms interaction times with those of gaseous CO_2. Gaseous CO_2 exhibits a characteristic vibronic peak at 292.75 eV that is not present for dissolved CO_2.

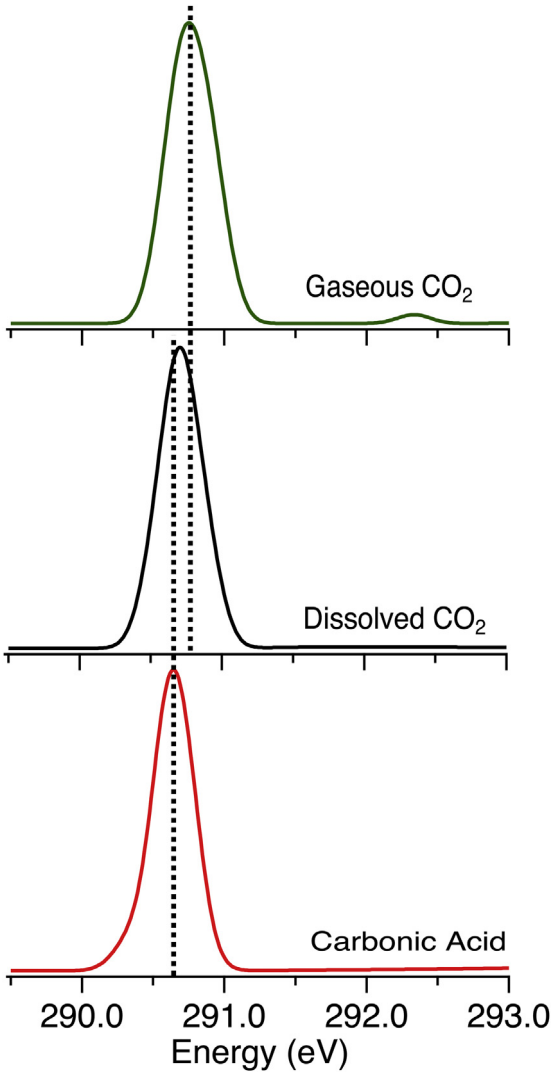

Figure 3. Calculated XAS spectra for aqueous carbonic acid (red), dissolved CO_2 (black), and gaseous CO_2 (green). A measurable blue shift is observed between the transition from carbonic acid to gaseous CO_2. Predicted peak maxima are at 290.64 eV (carbonic acid), 290.71 eV (dissolved CO_2), and 290.75 eV (gaseous CO_2). (For interpretation of the references to color in this figure legend, the reader is referred to the web version of this article.)

functions (RDFs) for the carbonyl oxygen (=O) to water hydrogen (H_w) distances for dissolved CO_2 and H_2CO_3 are shown in Figure 4A. A shift of the first peak in the RDF to a longer distance in CO_2 indicates a weaker interaction between the CO_2 carbonyl oxygens and the water hydrogens relative to that of H_2CO_3. The C–O_w RDFs for CO_2 and H_2CO_3 (Figure 4B) both show a broad peak around 3–5 Å. The onset of this broad feature is shifted to shorter distances for hydrated CO_2 relative to that of H_2CO_3 indicating a stronger interaction between the CO_2 carbon and the water oxygens. This C–O_w interaction is a prerequisite for the hydrolysis of dissolved CO_2 to form carbonic acid, bicarbonate, and carbonate [34]. While the RDFs between the water oxygens (O_w) of aqueous CO_2 and H_2CO_3, shown in Figure 5, are not significantly different from that of pure water, the RDFs of both CO_2 and H_2CO_3 of exhibit a higher first maximum and a lower first minimum, indicating a more ordered liquid structure surrounding the solute. This result is in general agreement with predictions made by Kumar et al. wherein CO_2 was predicted to behave as a typical hydrophobic, solute carving out a cylindrical void which enhances the tetrahedral hydrogen bond network of the surrounding solvent [17].

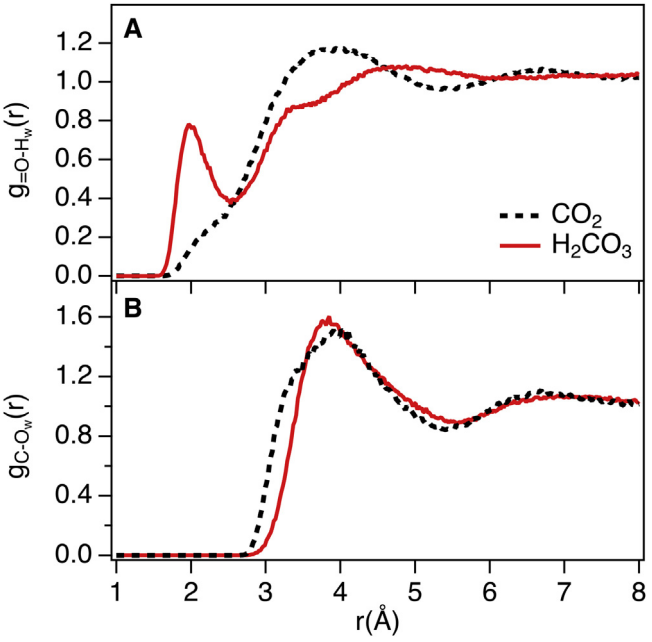

Figure 4. Calculated radial distribution functions for aqueous carbonic acid (red) and dissolved carbon dioxide (dashed black). The labels =O, and C refer to the carbonyl oxygen and carbon respectively. O_w and H_w refer to the oxygens and hydrogens of the water molecules. Bin sizes are 0.02 Å in all cases. (For interpretation of the references to color in this figure legend, the reader is referred to the web version of this article.)

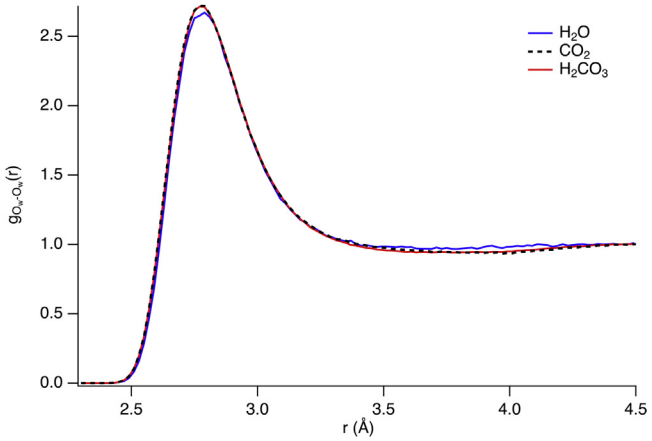

Figure 5. Calculated oxygen–oxygen radial distribution functions for pure TIP3P water and for water containing dissolved CO_2 or aqueous H_2CO_3. Both the RDFs of CO_2 and H_2CO_2 exhibit slightly higher first maxima and lower first minima indicating a more ordered liquid structure surrounding the solute. Bin sizes are 0.02 Å in all cases.

4. Conclusions

This first characterization of dissolved carbon dioxide under ambient conditions by X-ray absorption spectroscopy and first principles XCH calculations establishes the detailed hydration properties of dissolved carbon dioxide. Calculated spectral energy shifts and intensities between aqueous carbonic acid, dissolved carbon dioxide, and gaseous carbon dioxide correspond well with experimentally measured spectra. In future studies, we will focus on resolving some limitations of our current experimental design (i.e. finer control over the liquid interaction times) and the limitations of the molecular dynamics modeling through the implementation of higher level *ab initio* theories.

Acknowledgments

This work was supported by the Director, Office of Basic Energy Sciences, Office of Science, U.S. Department of Energy (DOE) under Contract No. DE-AC02-05CH11231, through LBNL Chemical Sciences Division. Molecular dynamics and X-ray spectral simulations were performed with D.P. as part of a User Project at The Molecular Foundry, Lawrence Berkeley National Laboratory (LBNL). Computational resources were provided by the National Energy Research Scientific Computing Center (NERSC), a DOE Advanced Scientific Computing Research User Facility for calculating X-ray spectra. Molecular dynamics simulations were performed using the computational resources of the Molecular Graphics and Computation Facility in the UC Berkeley College of Chemistry (NSF CHE-0840505). The authors thank Wanli Yang and Jon Spear for beamline support at the Advanced Light Source. The data presented are available upon request to saykally@berkeley.edu.

References

[1] A. Putnis, Science 343 (6178) (2014) 1441.
[2] H.A. Al-Hosney, V.H. Grassian, J. Am. Chem. Soc. 126 (26) (2004) 8068.
[3] A. Ridgwell, R.E. Zeebe, Earth Planet. Sci. Lett. 234 (3–4) (2005) 299.
[4] D. Kikeri, M.L. Zeidel, B.J. Ballermann, B.M. Brenner, S.C. Hebert, Am. J. Physiol. 259 (3 Pt 1) (1990) C471.
[5] Y. Abe, A. Iizuka, H. Nagasawa, A. Yamasaki, Y. Yanagisawa, Chem. Eng. Res. Des. 91 (5) (2013) 933.
[6] R.K. Dash, J.B. Bassingthwaighte, Ann. Biomed. Eng. 34 (7) (2006) 1129.
[7] K. Maher, C.P. Chamberlain, Science 343 (6178) (2014) 1502.
[8] M. Garcia-Rios, J. Cama, L. Luquot, J.M. Soler, Chem. Geol. 383 (2014) 107.
[9] Y.-S. Choi, S. Nesic, D. Young, Environ. Sci. Technol. 44 (23) (2010) 9233.
[10] P.M. Haugan, H. Drange, Energy Convers. Manag. 37 (6–8) (1996) 1019.
[11] O. Hoegh-Guldberg, P.J. Mumby, A.J. Hooten, R.S. Steneck, P. Greenfield, E. Gomez, C.D. Harvell, P.F. Sale, A.J. Edwards, K. Caldeira, et al., Science 318 (5857) (2007) 1737.
[12] J.C. Orr, V.J. Fabry, O. Aumont, L. Bopp, S.C. Doney, R.A. Feely, A. Gnanadesikan, N. Gruber, A. Ishida, F. Joos, et al., Nature 437 (7059) (2005) 681.
[13] K. Caldeira, M.E. Wickett, Nature 425 (6956) (2003) 365.
[14] S.K. Reddy, S. Balasubramanian, Chem. Commun. 50 (5) (2014) 503.
[15] F.J.J. Buytendyk, R. Brinkman, H.W. Mook, Biochem. J. 21 (3) (1927) 576.
[16] A.L. Soli, R.H. Byrne, Mar. Chem. 78 (2–3) (2002) 65.
[17] P.P. Kumar, A.G. Kalinichev, R.J. Kirkpatrick, J. Phys. Chem. B 113 (3) (2008) 794.
[18] X. Wang, W. Conway, R. Burns, N. McCann, M. Maeder, J. Phys. Chem. A 114 (4) (2010) 1734.
[19] Y. Pocker, D.W. Bjorkquist, J. Am. Chem. Soc. 99 (20) (1977) 6537.
[20] T.M. Abbott, G.W. Buchanan, P. Kruus, K.C. Lee, Can. J. Chem. 60 (8) (1982) 1000.
[21] J. Baltrusaitis, V.H. Grassian, J. Phys. Chem. A 114 (6) (2010) 2350.
[22] K. Adamczyk, M. Premont-Schwarz, D. Pines, E. Pines, E.T.J. Nibbering, Science 326 (5960) (2009) 1690.
[23] H. Falcke, S.H. Eberle, Water Res. 24 (6) (1990) 685.
[24] C.S. Tautermann, A.F. Voegele, T. Loerting, I. Kohl, A. Hallbrucker, E. Mayer, K.R. Liedl, Chemistry 8 (1) (2002) 66.
[25] R.C. Patel, R.J. Boe, G. Atkinson, J. Solut. Chem. 2 (4) (1973) 357.
[26] K.I. Peterson, W. Klemperer, J. Chem. Phys. 80 (6) (1984) 2439.
[27] A. Stirling, J. Phys. Chem. B 115 (49) (2011) 14683.
[28] M. In Het Panhuis, C.H. Patterson, R.M. Lynden-Bell, Mol. Phys. 94 (6) (1998) 963.
[29] M. Galib, G. Hanna, Phys. Chem. Chem. Phys. 16 (46) (2014) 25573.
[30] K. Leung, I.M.B. Nielsen, I. Kurtz, J. Phys. Chem. B 111 (17) (2007) 4453.
[31] S.T. Moin, A.B. Pribil, L.H. Lim, V. Hofer, T.S. Randolf, B.R. Rode B.M., Int. J. Quantum Chem. 111 (7–8) (2011) 1370.
[32] S.T. Moin, A.K.H. Weiss, B.M. Rode, Comput. Theor. Chem. 1034 (2014) 85.
[33] V. Vchirawongkwin, A.B. Pribil, B.M. Rode, J. Comput. Chem. 31 (2) (2010) 249.
[34] G.A. Gallet, F. Pietrucci, W. Andreoni, J. Chem. Theory Comput. 8 (11) (2012) 4029.
[35] M. Prakash, V. Subramanian, S.R. Gadre, J. Phys. Chem. A 113 (44) (2009) 12260.
[36] B. Wang, Z. Cao, J. Comput. Chem. 34 (5) (2013) 372.
[37] A.H. England, A.M. Duffin, C.P. Schwartz, J.S. Uejio, D. Prendergast, R.J. Saykally, Chem. Phys. Lett. 514 (4–6) (2011) 187.
[38] M. Eigen, Angew. Chem. Int. Ed. Engl. 3 (1) (1964) 1.
[39] R.K. Lam, A.H. England, A.T. Sheardy, O. Shih, J.W. Smith, A.M. Rizzuto, D. Prendergast, R.J. Saykally, Chem. Phys. Lett. 614 (2014) 282.
[40] K.R. Wilson, B.S. Rude, J. Smith, C. Cappa, D.T. Co, R.D. Schaller, M. Larsson, T. Catalano, R.J. Saykally, Rev. Sci. Instrum. 75 (3) (2004) 725.
[41] D.A. Case, T.A. Darden, Cheatham, C.L. Simmerling, J. Wang, R.E. Duke, R. Luo, K.M. Merz, D.A. Pearlman, M. Crowley, R.C. Walker, W. Zhang, B. Wang, S. Hayik, A. Roitberg, G. Seabra, K.F. Wong, F. Paesani, X. Wu, S. Brozell, V. Tsui, H. Gohlke, L. Yang, C. Tan, J. Mongan, V. Hornak, G. Cui, P. Beroza, D.H. Mathews, C. Schafmeister, W.S. Ross, P.A. Kollman, Amber 9, University of California, San Francisco, 2006.
[42] D. Prendergast, G. Galli, Phys. Rev. Lett. 96 (21) (2006) 215502.
[43] P. Giannozzi, S. Baroni, N. Bonini, M. Calandra, R. Car, C. Cavazzoni, D. Ceresoli, G.L. Chiarotti, M. Cococcioni, I. Dabo, et al., J. Phys.: Condens. Matter 21 (39) (2009) 395502.
[44] J.P. Perdew, K. Burke, M. Ernzerhof, Phys. Rev. Lett. 77 (18) (1996) 3865.
[45] W. Humphrey, A. Dalke, K.V.M.D. Schulten, J. Mol. Graph. 14 (1) (1996) 33.
[46] D. Vanderbilt, Phys. Rev. B 41 (Rapid Communications) (1990) 7892.